AD-A253 125

1. AGENCY USE ONLY (Leave blank)	2. REPORT DATE	3. REPORT TYPE AND DATES COVERED
	June 30, 1992	Quarterly 30 June 91 30 September 91

4. TITLE AND SUBTITLE
Optoelectronic Materials Center, A Collaborative Program Including University of New Mexico, Stanford University and California Institute of Technology

5. FUNDING NUMBERS
(2)
MDA972-90-C-0046

6. AUTHOR(S)
S.R.J. Brueck, Editor

7. PERFORMING ORGANIZATION NAME(S) AND ADDRESS(ES)
University of New Mexico
Center for High Technology Materials
EECE Building, Room 125
Albuquerque, NM 87131

8. PERFORMING ORGANIZATION REPORT NUMBER
Qtr

9. SPONSORING/MONITORING AGENCY NAME(S) AND ADDRESS(ES)
Defense Advanced Research Projects Agency
ARPA Order No. 7526 Issued by DARPA/CNMO
under Contract #MDA972-90-C-0046

10. SPONSORING/MONITORING AGENCY REPORT NUMBER

11. SUPPLEMENTARY NOTES

12a. DISTRIBUTION/AVAILABILITY STATEMENT
This document has been approved for public release and sale; its distribution is unlimited.

12b. DISTRIBUTION CODE

13. ABSTRACT (Maximum 200 words)

The Optoelectronic Materials Center is a collaborative program involving the University of New Mexico, Stanford University, and the California Institute of Technology. Sandia National Laboratories and MIT Lincoln Laboratory are also involved in this program under separate contract vehicles. This program emphasizes three main areas:

diode-based visible sources
two-dimensional optical interconnects, and
high-speed optoelectronics.

Progress on individual tasks is very briefly discussed below. Several of the tasks will impact more than one of the above areas. For simplicity, the tasks are arranged by institution in an order roughly determined by the above areas.

14. SUBJECT TERMS	15. NUMBER OF PAGES
Diode based visible sources, two dimensional optical interconnects, High speed Optoelectronics.	16. PRICE CODE

17. SECURITY CLASSIFICATION OF REPORT	18. SECURITY CLASSIFICATION OF THIS PAGE	19. SECURITY CLASSIFICATION OF ABSTRACT	20. LIMITATION OF ABSTRACT
	Unclassified	Unclassified	

Sponsored by

DEFENSE ADVANCED RESEARCH PROJECTS AGENCY

OPTOELECTRONICS MATERIAL CENTER

A Collaborative Program including

Center for High Technology Materials
of the University of New Mexico

Stanford University

California Institute of Technology

ARPA Order No. 7526
Issued by DARPA/CMO under contract #MDA972-90-C-0046

DARPA QUARTERLY STATUS REPORT

Period ending Sept. 30, 1991.

UNIVERSITY OF NEW MEXICO -
CENTER FOR HIGH TECHNOLOGY MATERIALS

Visible Diode Lasers

Facilities and Equipment -

Extension to Crystal Growth Facility

In collaboration with Westwork Architects P.A., we are preparing a construction plan for the extension to the Crystal Growth Facility. The design emulates major features of the existing building and we estimate completion in July 1992. We have copied the existing facility for two reasons: First, for employee safety, the facility response to alarm conditions will be the same in each half of the existing facility. Secondly, the existing facility design has been road-tested and has the confidence and approval of UNM and the emergency support agencies (Fire Dept., Police, Medical Services).

New MOCVD Reactor

We are currently defining the specifications for the new MOCVD reactor. The new reactor design is based on our existing horizontal-geometry system but will incorporate many improvements. These improvements are necessary to maintain a state-of-the-art MOCVD growth capability that can meet the challenging requirements of advanced optoelectronic devices:

Wafer rotation: This will improve layer thickness and compositional uniformity ideally to better than 0.5% variation across a three-inch wafer.

Automatic pressure control: The manual pressure control valve currently used for pressure control on each metalorganic bubbler will be replaced by an automatic valve and controller. This will improve pressure stability, which directly effects the reproducibility of growth rate and composition. Automatic pressure control will be particularly beneficial during the growth of graded hetero-interfaces, for example, in VCSEL mirror layers or HBT base emitter junctions.

Streamlined LN Cold Trap: The liquid nitrogen cold-trap that traps reaction waste (downstream of the reaction zone) will be streamlined and moved downstream of the reactor tube, to reduce the backstreaming of particles. In the present system these fine particles are adsorbed onto the trap but can be released when they are disturbed by flow transients or by a non-laminar gas flow over the trap.

Bakeout heaters: The present system of heater tapes, which are wound around the system plumbing, will be replaced by a more convenient heating medium.

Glove Box: A high integrity glove box will be incorporated into the new reactor, to avoid all contamination of the open reaction tube and sample by air during loading and unloading operations.

In preparation for the new reactor, staff at the Crystal Growth Facility will upgrade the existing reactor control software. The new software will incorporate global variables that are shared between each subroutine and will avoid the necessity of manual key entry between the calculation, generation, and run phases of the growth sequence. This software will also be retrofittable on the existing MOCVD reactor.

After meetings and discussions with many different MOCVD vendors, we judge the following as potentially having the expertise required to deliver a state-of-the-art MOCVD system. When the RFP is completed it will be distributed to these vendors in addition to our normal contracting practices of advertising for bids.

Aixtron (Germany)
Caleb (USA)
CVT (UK)
Epiquip (Sweden)
Emcore (USA)
Spire (USA)
Thomas Swann Ltd. (UK)
MR Semicon (UK)

MOCVD Growth

Improved Calibration Schedule for VCSEL Growth

The vertical cavity surface emitting laser (VCSEL) is a highly complex structure consisting of typically more than 80 layers divided into an upper and lower mirror region with a central quantum well active region. Before the growth of this device a calibration procedure is necessary to ensure that the growth rate (and thickness of each layer) and the AlGaAs and InGaAs alloy compositions, are accurately known. This calibration is essential in the VCSEL structure as the optical thickness of each layer must be accurate to within 0.5%.

We have observed that there is a slow drift of growth rate with time (typically 1% per week) so that if we take too long calibrating, the final VCSEL structure can miss the target thickness. This is a key problem, which seriously affects the yield of VCSEL wafers and could prejudice any future commercialization of this device. We are therefore rethinking our calibration procedure and believe that we can reduce it to only three growths. This new approach will be tested and described in the next quarterly report.

Regrowth

We have continued to develop a regrowth technology for the integration of lenses in unstable resonator type devices. In fact, a successful regrowth technology will have a much wider application than just in this device as it will be an important step towards the monolithic integration of different device functions by selective epitaxy.

The principle of regrowth is simple and consists of an initial growth step, then an ex-situ photolithography/etching step and finally the sample is reintroduced into the MOCVD reactor for a second growth step. The quality of the second growth (and

generally the subsequent device performance) is critically dependent on the condition of the surface that is left after the photolithography/etching step.

We have evaluated several surface treatments by examining the electrical and optical quality of regrown interfaces with $Al_xGa_{1-x}As$ compositions in the range $0<x<0.6$. These surface treatments included: ex-situ surface passivation with inorganic sulfides, *in-situ* heat treatment, and *in-situ* HCl etching.

We obtained the highest quality regrown interfaces using a combined treatment involving an ex-situ ammonium sulfide passivation and an in-situ HCl etch. We will further test this surface treatment by using Ti in a regrown laser structure.

Doping

This quarter we have made good progress towards the development of p-type and n-type doping suitable for the optically driven pnpn switch structure that will eventually be grown on top of the VCSEL. The pnpn device structure requires a high p-type doping in the emitter to achieve a good current gain. Furthermore, the p-n junctions must be accurately located at the heterojunctions for a good injection efficiency. Any diffusion of the dopant will dramatically reduce this efficiency.

For p-type doping, we evaluated zinc (from a source of diethylzinc, DEZn) and carbon (from a dilute mixture of CCl_4 in hydrogen). For n-type doping, tellurium (from a source of diethyltelluride) was used.

Zinc diffuses heavily at high doping levels making it unsuitable for these structures. Carbon does not appear to diffuse, confirming results obtained from MBE and MOMBE work. However, our current carbon source is too dilute to allow the required p+ concentrations to be achieved. We will continue these carbon doping experiments using a source of pure CCl_4

<u>Optical Switches and Logic Gates Based on VCSELs</u>

Smart pixels based on vertical-cavity surface-emitting lasers (VCSELs) are potentially competitive with, and are in many respects superior to, those based on spatial light modulators (SLMs) such as the Self Electro-Optic Effect Device (SEED). Optical switches based on SEEDs have relatively low optical contrast and require an external optical source array. Optical switches based on VCSELs, on the other hand, have a built-in source with high output power and optical contrast. The VCSELs strengths include its superior power efficiency, low beam divergence, good modal characteristics, high speed, high optical contrast (between lasing and spontaneous emission levels), high output power, and their inherent threshold behavior. These qualities are well-suited for a two-dimensional array of cascadable, optical threshold switches.

An optical switch based on the monolithic integration of a heterojunction phototransistor (HPT) and a VCSEL has been demonstrated. A high gain HPT (β = 200) can amplify the photocurrent induced by a relatively low input optical power (<100 μW) to provide a collector current of several mA, which is sufficient to drive a well-designed VCSEL above its lasing threshold. Thus, with the VCSEL and HPT biased in series, a low optical input to the HPT can switch-on the VCSEL from its quiescent (dark) state, which is characterized by weak spontaneous emission, to a lasing state characterized by a large output power, thus achieving a significant optical gain. The lasing threshold of the VCSEL provides a threshold for the optical switching characteristic. In the previous quarters, we have demonstrated a hybrid HPT/VCSEL optical switch with a differential

optical gain of 200, an overall optical gain of 20, an optical contrast of 1700, and an output power of 2 mW. We have now achieved a monolithic HPT/VCSEL optical switch with an overall optical gain of 10, an optical contrast of 1000, an optical switching threshold of 27 μW, and a thermal-limited optical output of 0.3 mW. This is the first experimental demonstration of a monolithic HPT/VCSEL switch that is optically cascadable (in contrast to the Bellcore switch). The energy required to effect switching is about 5-6 picojoules.

Progress was also made in developing high gain HPTs (gain >200) and photothyristors with strongly latching characteristics. These devices were grown in-house using MOCVD, and will be combined monolithically with VCSELs shortly to produce a latching optical switch.

Because of the advances that we have made in improving the electrical characteristics of VCSELs, the successful demonstration of their monolithic integration with HPTs, and the achievement of good optical switching characteristics, we have decided that this is a more promising approach for us to pursue in our quest for a smart pixel than the SLM (SEED)-based approach we had previously proposed. Thus we will be redirecting our future efforts, shifting the emphasis of our research program from SLMs to VCSELs, which we believe to be a more versatile technology with broader capabilities than the one based on SLMs. (J. Cheng)

Surface Normal Visible Second Harmonic Generation in Waveguides.

Status

During this quarter we succeeded in demonstrating the counterpropagating surface normal second harmonic generation in a single layer GaAs waveguide. The waveguide consisted of a 400Jnm GaAs layer on top of a thick Al(0.3)Ga(0.7)As cladding layer. A 3 micrometer ridge was defined photolithographically using wet chemical etching. A Nd:YAG laser laser at 1.064 micrometers with 100 ps pulses at a repetition rate of 82MHz and an average power of 75mW was coupled into the waveguide using a quarter waveplate to adjust the polarization. The interference between the counterpropagating TE and TM modes could clearly be observed with dimmed room lights. By measuring the fundamental power at the output facet, we estimated the average power power in the waveguide at 300 microwatts. Using a photomultiplier, the average SH power was estimated to be 10 pW with a Si3N4 AR coating on the top surface, but no corrections made for losses in the collection optics.

Plans

Our studies have shown us that materials transparent to the second harmonic will always have a disadvantage when used in counterpropagating SHG when compared with copropagation coupled with quasi-phase matching. Considering the experimental difficulties of producing PLZT waveguides and of poling PLZT, the rest of this program will be devoted to compound semiconductor studies and our investigations into PLZT will cease.

No changes in personnel. (Malloy)

Novel Quantum Mechanical Effects of Semiconductor Structures Including Shaped- and Coupled-quantum Wells

The analysis has been extended to GaAs/$Al_xGa_{1-x}As$ superlattices. We have investigated the effects of superlattice parameters, such as subband index, thicknesses of both constituent materials, and barrier height (composition) on the shifts of subband-edge energy, between the two extreme cases of operator ordering. Conditions have been identified where optical transition energy is highly sensitive on operator ordering.

In the next quarter we plan to use available experimental data to establish the most plausible operator ordering. (M. Osinski)

Design, Fabrication, and Characterization of Electrically Pumped, AlGaAs and InGaAs-based, Vertical-Cavity, Surface-Emitting Lasers with the Goal of Room Temperature, Continuous Wave Operation at an Output Power 1 mW or Greater.

Thermal properties have been investigated for etched-well VCSELs of various active-region diameters, using a self-consistent thermal-electrical analysis.

In the next quarter we plan to develop a thermal model of planar top-surface-emitting proton-implanted VCSELs. (M. Osinski)

Investigation of High-Power Pulsed Lasers, Especially Ultrashort Pulse Devices and Giant-Pulse, Quasi-CW Lasers

Measurements of peak optical power density have been performed on optically pumped DFB-RPG lasers. A record-high power density of 4.5 MW/cm^2 has been obtained.

In the next quarter we plan to perform a TEM study of MOCVD-grown DFB-RPG wafers. (M. Osinski)

Demonstration of Electrical Modulation of Individual Surface-Emitting Lasers in a Two-Dimensional Array Format and Study of the Feasibility of a Time-Multiplexed Matrix-Addressed Source Array

The results of 2-D array analysis indicate that thermal profiles within each emitter are skewed, which will break cylindrical symmetry of VCSEL resonators. This opens up a new possibility of thermally engineered asymmetric waveguides/antiguides that could in principle enhance the in-phase operation of the array. Lack of azimuthal symmetry in the central element of the array offers a promise of polarization control.

In the next quarter we palm to extend the analysis to large-size ("infinite") two-dimensional arrays. (M. Osinski)

CALIFORNIA INSTITUTE OF TECHNOLOGY

Dislocation Density Reduction and Island Suppression in Epitaxial Ge Growth on Si by Ion-Assisted Molecular Beam Epitaxy

Currently there is considerable interest in misfit accommodation in heteroepitaxy for integration of device-quality III-V and II-VI films with Si integrated circuit technology. Despite many advances, no process has yet demonstrated adequate control of misfit

dislocations. Of particular interest is the control of misfit accommodation that results in either: (1) smooth, coherently strained layers; and (2) reduction or elimination of defects from the *active* region, possibly at the expense of defect creation elsewhere in the film. Ion-assisted molecular beam epitaxy is one of a class of techniques that allow modification growth kinetics during heteroepitaxy, with the potential for novel means of misfit accommodation.

In the last quarter, using ion-assisted molecular beam epitaxy, we have demonstrated:

1. Reduction of dislocation density in thick Ge growth on Si by a factor of four.

2. Suppression of island formation during heteroepitaxy of thin films with large misfit (4.2 %).

We have observed a reduction of the threading dislocation density in the Ge films grown on Si in a two-step process with (1) 30 nm Ge film grown at 300° C (growth-rate limited regime) with 200 eV low energy ion bombardment and annealed at 550° C for 30 min. and (2) 320 nm Ge film grown at 550° C on top of the annealed buffer layer, compared with 350 nm Ge film grown at 550° C. In typical two-step growth, the buffer layers are annealed at temperatures higher than the final film growth temperature, while in this process, the maximum temperature used was the final growth temperature. The threading dislocation density is reduced by a factor of approximately 5 as compared with similarly-processed thermal-growth samples.

We have also investigated suppression of the Ge island formation on Si using low energy ion bombardment during growth. The films bombarded by the low energy ion beam (70-150 eV, with ion-to-atom flux ratio in the range of 0.01 to 0.2) grow in a layer-by-layer mode up to 3 nm, whereas islanding occurs for thermally grown films at a thickness of 1 nm. The driving force for islanding still exists; as films smooth, coherent films grown at 400° C exhibit island formation upon annealing at 600° C. This suggests that the film is coherently strained, and that low energy ion bombardment results in dynamic dissociation of incipient islands during the early stages of growth. (H. A. Atwater)

<u>Nanometer-Scale Selective Growth of GaAs and InGaAs by OMVPE and Application to Quantum Size Effect Semiconductor Lasers</u>

There is currently great interest in the fabrication of structures that are two and three dimensional analogs of the conventional quantum well. Several potential applications of arrays of such structures have been proposed, including diode laser active layers and new nonlinear optical materials. Key problems involved in successfully applying these structures in devices are interface quality and abruptness, structural uniformity, and, for application to lasers, ability to pump the structures efficiently without leakage effects dominating. Selective growth is a potential candidate for fabricating highly uniform nanostructures and for providing extremely good built-in current blocking capability that could be exploited in ultra-low threshold conventional quantum-well laser diodes.

A novel extension of selective epitaxy, facet modulation selective epitaxy, has been applied successfully to quantum-well wire doublet fabrication in the $Al_xGa_{1-x}As$ material system. Facet modulation selective epitaxy is the application of different precursor chemistries to layers within single growth to alter sequentially the appearance of facets on a growing structure and to thereby form heterostructures of novel geometry.

The smallest wires fabricated by applying facet modulation selective epitaxy have crescent cross sections less than 140 Å thick and less than 1400 Å wide. Low temperature (liquid nitrogen and liquid helium temperatures) cathodoluminescence analysis and cross-sectional transmission electron microscopy were performed to determine the luminescence properties and the approximate dimensions of these wires.

Detailed results will be presented in a paper accepted for publication in the January 13, 1992 issue of the Applied Physics Letters. The paper is titled: *Facet modulation selective epitaxy--a technique for quantum-well wire doublet fabrication.*

Thick (>1000 Å) multilayer GaAs-AlGaAs selectively grown heterostructures also have been characterized by scanning electron microscopy, backscattered electron microscopy, and spectrally-resolved cathodoluminescence analysis. Different facet-dependent growth rates of the GaAs and AlGaAs layers were observed.

Further size reduction of the wire doublets grown by facet modulation selective epitaxy will be pursued by reducing the width of the starting $Al_xGa_{1-x}As$ facets and the amount of GaAs deposited. By doping the layers above and below the wire, doublet p-type and n-type respectively, and by embedding the wire doublet in an $Al_xGa_{1-x}As$ optical waveguide, an injection laser may be fabricated. Other applications will also be explored, including the fabrication of quantum dots and the extensions of this technique to other material systems besides $Al_xGa_{1-x}As$, such as $In_xGa_{1-x}As$. (K. Vahala)

Ultra-low Threshold Semiconductor Lasers

Processed epitaxial layers into low threshold buried heterostructures using wet etching and a two step regrowth process by Liquid Phase Epitaxy (LPE). The active region width is 1.5 - 2 μm. Lasers with as-cleaved mirrors were tested for threshold current as a function of cavity length as shown in Figure 1. The results are compared with single quantum well material grown by Molecular Beam Epitaxy (MBE) previously. The optimum cavity length decreases with the increasing number of quantum wells as was expected. This length ranged from above 300 lm for the single well to about 100 μm for the triple well. Minimum observed threshold currents (CW) are 2.8 mA, 1.0 mA, and 1.6 mA for the single, double and triple quantum well lasers, respectively. The lasers operate in a single lateral mode with a far field divergence angle of 25 degrees. For 150 μm long lasers we are able to measure over 40 mW CW power per facet at room temperature.

We plan to investigate dislocation density reduction by enhancing the threading dislocation mobility in graded epitaxial buffer layers. We will also investigate GaAs and ZnTe growth on the substrates with pure Ge and graded buffer layers. (A. Yariv)

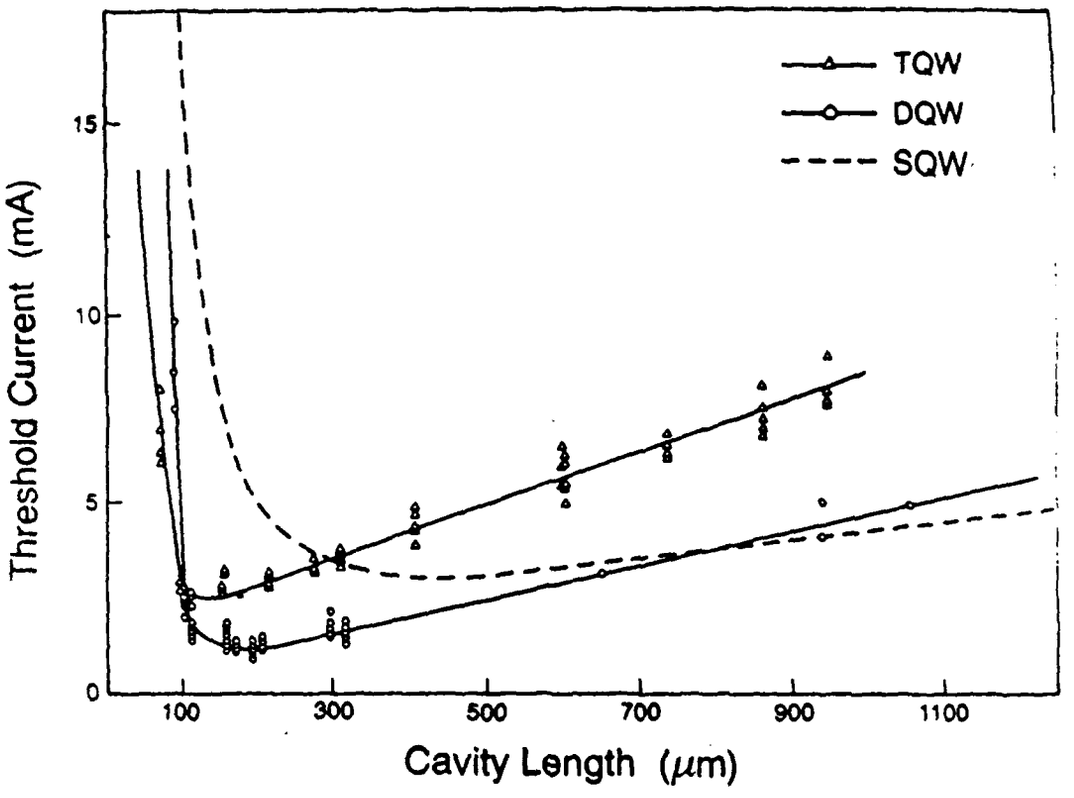

Figure 1. Uncoated BH SQW, DQW, TQW Lasers

Massively Parallel Optical Networks

In extending our work on optoelectronic GaAs neuron circuits for neural network applications, we have gone from circuits with a single optical input and electrically set thresholds to a circuit with two optical inputs. With this new circuit the threshold can be set optically, eliminating bottlenecks from electrical inputs. The circuit can also be used to implement bipolar weights in an optical neural network, In an incoherent optical system, the photodetectors detect the intensity of the light, a unipolar signal. To implement bipolar weights, two photodetectors are required. So for our optoelectronic neuron circuit, we require the circuit to perform a nonlinear thresholding function on the difference of the two optical inputs. The optical circuit is shown in Figure 2.

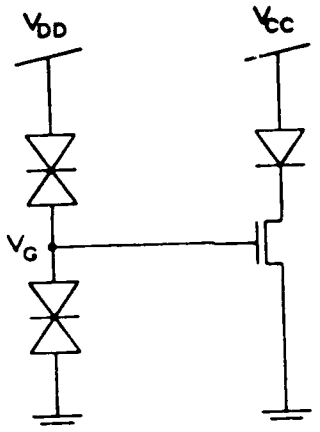

Figure 2. Optoelectronic Neuron Circuit Using MSM Photodetectors

To implement this circuit, we monolithically integrated two MSM (metal-semiconductor-metal) photodetectors with a driving MESFET and an LED. The cross-sectional view of the circuit is shown in Figure 3.

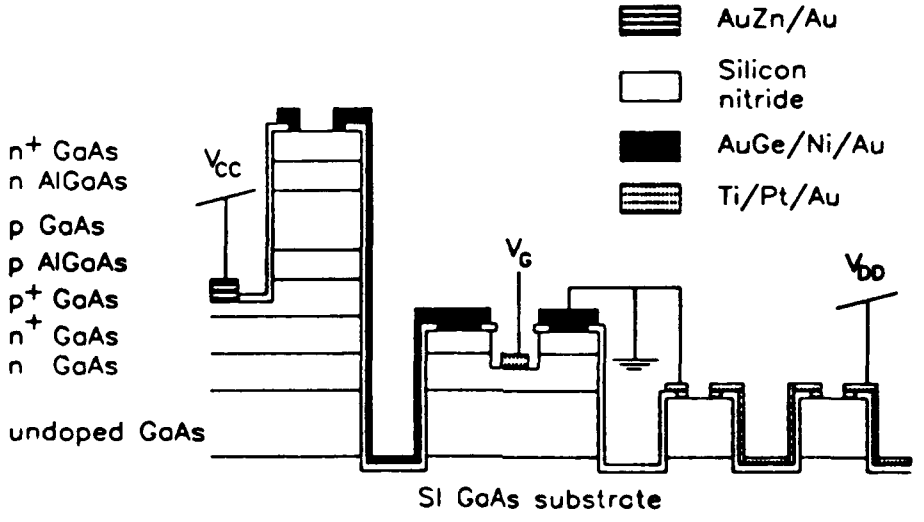

Figure 3. Cross-sectional View of the Monolithically Integrated Optoelectronic Circuit

The MSM detectors are fabricated by depositing interdigitated Schottky contacts (Ti/Pt/Au) on undoped GaAs. The exectrodes width was 4 μm with 6 μm spacing between electrodes. The total active area was 40 μm x 40 μm. Although the MSM detectors do not have the current gain that optical FETs have, they are very easy to fabricate, not sensitive to etch nonuniformities, and have very low dark currents. Typical detection response for MSM detectors is .2A/W. A photomicrograph of the fabricated circuit is shown in Figure 4.

Figure 4. Photomicrograph of the MSM Optoelectronic Circuit

The circuit characteristics are shown in Figure 5. The current through the LED is plotted in the vertical axis. Experimentally it is much easier and more reliable to measure the current rather than using a photodetector to measure the light out of the LED. One can calculate the power from the LED efficiency ($\approx$ .01 W/A). The figure shows curves for various fixed optical powers on the lower detector (P_2). The circuit switches when the optical inputs are equal. Thus the lower detector is acting as a threshold for the circuit.

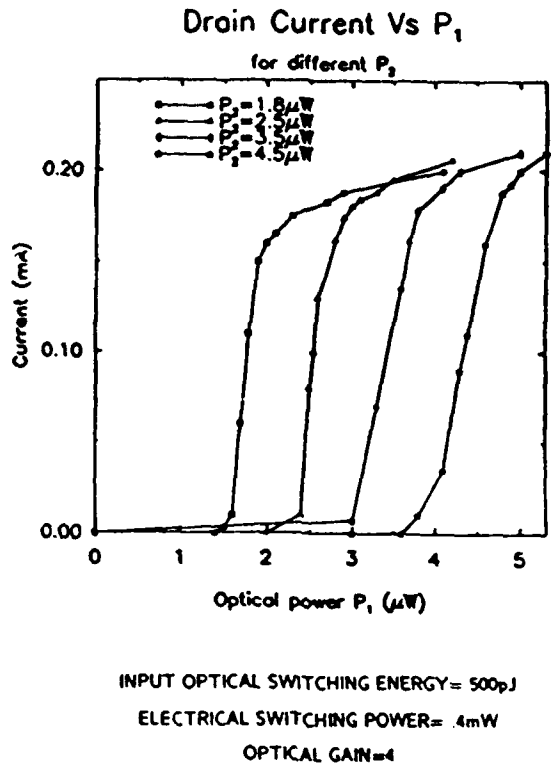

Figure 5. Output Characteristics of the MSM Optoelectronic Circuit

Figure 6 shows the circuit response plotted against the difference in the two optical powers, P_1-P_2. We see that the curves are all fairly symmetrical about zero. This circuit requires a differential optical power of .5 μW to switch the LED on. The optical power out of the LED was 2 μW with a power dissipation of 1 mW.

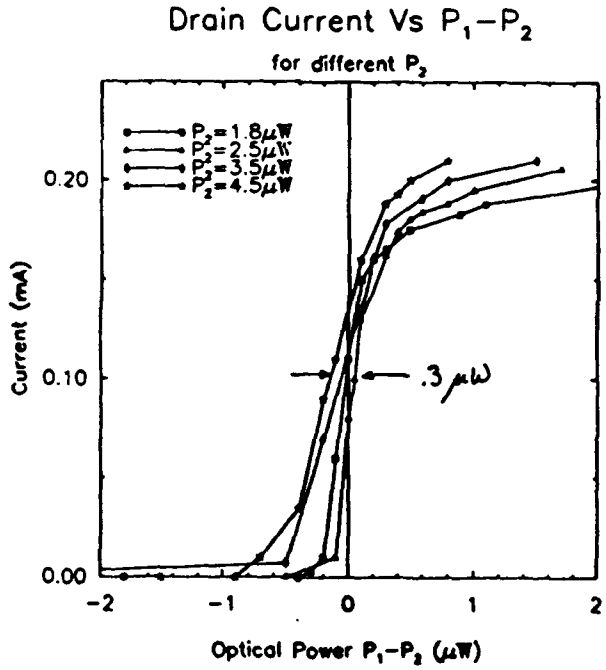

Figure 6. Circuit Response as a Function of the Difference in the Two Optical Input Powers

Although this circuit does not have as large optical gain or sensitivity as the optical FET-based circuit, this circuit was very easy to fabricate and shows that the threshold could be set optically. By using two optical FETs rather than MSM detectors, we should be able to increase the sensitivity and increase the optical gain. Because the dark current, gain, and saturation voltage of an optical FET are affected by its dimensions and gate recess, further analysis needs to be made before a two optical input circuit using optical FETs can be realized. (D. Psaltis)

Papers and Presentations

Papers Submitted

M. Mahbobzadeh, E. Gandjbakhch, E. A. Armour, K. Zheng, S.-Z. Sun, C. F. Schaus, and M. Osinski, *Distributed-feedback GaAs/AlGaAs/AlAs vertical-cavity surface-emitting laser with resonant-periodic gain active region*, 3rd Annual Symp. on Ceramics & Advanced Materials, Albuquerque, NM, Oct. 24-25, 1991.

M. Mahbobzadeh, E. Gandjbakhch, E. A. Armour, K. Zheng, S.-Z. Sun, C. F. Schaus, and M. Osinski, *Distributed-feedback vertical-cavity surface-emitting laser with resonant-periodic-gain active region*, Laser Diode Technology & Applications IV, SPIE Laser & Sensor Engineering Symp., OE/LASE'92, Los Angeles, CA, Jan. 19-24, 1992.

M. Mojahedie and M. Osinski, *Operator ordering in effective-mass Hamiltonian for semiconductor superlattices and quantum wells*, 3rd Annual Symp. on Ceramics & Advanced Materials, Albuquerque, NM, Oct. 24-25, 1991.

W. Nakwaski and M. Osinski, *Thermal properties of etched-well GaAs/AlGaAs surface-emitting diode lasers*, 3rd Annual Symp. on Ceramics & Advanced Materials, Albuquerque, NM, Oct. 24-25, 1991.

M. Osinski and W. Nakwaski, *Thermal properties of etched-well surface-emitting diode lasers and two-dimensional arrays*, Laser Diode Technology & Applications IV, SPIE Laser & Sensor Engineering Symp., OE/LASE'92, Los Angeles, CA, Jan. 19-24, 1992.

Papers Accepted

M. Mojahedie and M. Osinski, *Effects of operator ordering in effective-mass Hamiltonian on transition energies in semiconductor quantum wells*, OSA 1991 Annual Meeting, San Jose, CA, Nov. 3-8, 1991.

W. Nakwaski and M. Osinski, *Thermal analysis of etched-well surface-emitting diode lasers*, Microwave & Optical Technology Lett.

W. Nakwaski and M. Osinski, *Heat source distribution in etched-well surface-emitting semiconductor lasers*, IEEE Photonics Technology Lett.

W. Nakwaski and M. Osinski, *Optimization of thermal properties of etched-well surface-emitting GaAs/AlGaAs diode lasers*, OSA 1991 Annual Meeting, San Jose, CA, Nov. 3-8, 1991.

W. Nakwaski and M. Osinski, *Thermal analysis of two-dimensional etched-well surface-emitting diode laser arrays*, IEEE LEOS 1991 Annual Meeting, San Jose, CA, Nov. 4-8, 1991.

Paper presented

M. Mahbobzadeh, E. Gandjbakhch, and M. Osinski, *High-power operation of distributed-feedback resonant-periodic-gain surface-emitting lasers*, accepted for Integrated Optoelectronics for Communication & Processing, SPIE Symp. on Optical Fiber Materials & Devices, OE/Fibers'91, Boston, MA, Sept. 3-6, 1991, Paper 1582-15.

Nakwaski and M. Osinski, *Improved thermal properties of etched-well surface-emitting lasers with highly-doped P-cladding*, accepted for Integrated Optoelectronics for Comm. & Processing, SPIE Symp. on Optical Fiber Materials & Dev., OE/Fibers'91, Boston, MA, Sept. 3-6, 1991, Paper 1582-33.